Title: Functional wiring of the human medial temporal lobe.

Authors: E. A. Solomon[1], J. M. Stein[2], S. Das[2], R. Gorniak[3], M. R. Sperling[4], G. Worrell[5], R. E. Gross[6], B. Lega[7], B. C. Jobst[8], D. S. Rizzuto[9], M. J. Kahana*[9].

Affiliations

[1]Department of Bioengineering, University of Pennsylvania, Philadelphia PA 19104, USA.
[2]Department of Radiology, Hospital of the University of Pennsylvania, Philadelphia PA 19104, USA.
[3]Department of Radiology, Thomas Jefferson University Hospital, Philadelphia PA 19107, USA.
[4]Department of Neurology, Thomas Jefferson University Hospital, Philadelphia, PA, 19107, USA
[5]Department of Neurology, Department of Physiology and Bioengineering, Mayo Clinic, Rochester, MN, 55905, USA
[6]Department of Neurosurgery, Emory School of Medicine, Atlanta GA 30322, USA.
[7]Department of Neurosurgery, University of Texas Southwestern, Dallas, TX, 75390, USA
[8]Department of Neurology, Dartmouth Medical Center, Lebanon, NH, 03756, USA
[9]Department of Psychology, University of Pennsylvania, Philadelphia, PA, 19104, USA

*Correspondence addressed to kahana@psych.upenn.edu

Abstract

The medial temporal lobe (MTL) is a locus of episodic memory in the human brain. It is comprised of cytologically distinct subregions that, in concert, give rise to successful encoding and retrieval of context-dependent memories. However, the functional connections between these subregions are poorly understood. To determine functional connectivity among MTL subregions, we had 108 subjects fitted with indwelling electrodes perform a verbal episodic memory task, and asked how encoding or retrieval correlated with coherence between regions. Here we report that coherent theta (4-8 Hz) activity underlies successful episodic memory, whereas high-frequencies exhibit significant desynchronization. During encoding, theta connections converge on the left entorhinal cortex, which concurrently exhibits an increase in high-frequency spectral power. Perirhinal cortex emerges as a hub of retrieval-associated theta connectivity, reflecting a substantial reorganization of the encoding-associated network. We

posit that coherent theta activity within the MTL marks periods of successful memory, but distinct patterns of connectivity dissociate key stages of memory processing.

Main Text

Storing episodic memory is an inherently integrative process, long conceptualized as a process that links information about new items to an observer's current thoughts, emotions, and environment[1]. Decades of behavioral observations, clinical case studies, and scalp electroencephalography (EEG) in humans have shed light on the key principles and diverse set of brain structures underlying this integration, including frontal, lateral temporal, and medial temporal cortex (MTL)[2]. Recent hypotheses invoke the idea that communication among these regions supports memory formation, spurred by a growing number of functional imaging and intracranial EEG (iEEG) experiments that show synchronized activity among the MTL and cortical structures during memory tasks[3–6].

However, the MTL has a unique role in supporting episodic memory. Damage to the MTL results in profound deficits of memory[7], and it has been shown to exhibit enhanced neural activity during memory processing in a range of tasks and experimental models[8,9], identifying this area as a key anatomic hub of episodic encoding and retrieval. The MTL is structurally complex; it is subdivided into hippocampus, rhinal cortex, and parahippocampal cortex. The cornu ammonis (CA), dentate gyrus, and subiculum comprise the hippocampus, while the entrorhinal and perirhinal cortices form rhinal cortex. Microscale recordings in animals have revealed that these substructures exhibit distinct patterns of activity during memory and navigation tasks, including the generation of oscillations, inter-regional synchronization, and neuronal selectivity for time and space[10–16]. Computational models of MTL function have

assigned unique roles to MTL substructures, pertaining to episodic encoding, retrieval, or recognition[10,17–20] – typically, these models suggest extrahippocampal regions are responsible for placing sensory inputs in a useful representational space, while the hippocampus itself forms associative links between these representations and their prevailing context.

Notably, virtually all of the aforementioned animal and modeling literature suggests that MTL substructures communicate with one another as they engage in memory processing. However, the volume of aforementioned work on intra-MTL connectivity has not been matched by validation studies in humans. Though a handful of investigations have begun to address this question in neurosurgical patients[21–23], limited electrode coverage and imprecise localizations have made it difficult to study the fine spatial scale and complete extent of neural synchronization within the MTL. But doing so is a crucial component of (1) confirming that intra-MTL synchronization observed in animal models also correlates with memory processing in humans, and (2) validating models of MTL function that suggest communication among specific regions – such as rhinal cortex versus hippocampus – supports computations necessary for associative memory formation and retrieval.

The use of intracranial depth electrodes to study neural activity in the MTL also allows neural activity to be studied at different timescales. Slow theta (4-8 Hz) oscillations in the hippocampus have been observed during memory processing in humans[24–27], as have fluctuations at higher frequencies, including the gamma (30-60 Hz) band[28,29]. These oscillations have been theorized to support synchronization between neural assemblies in the MTL[15,17,30–32], but MTL connectivity has not been fully mapped across frequency bands. The extent to which different frequencies underlie neural synchronization in memory therefore remains an open question,

though converging lines of evidence strongly suggest the most prominent connectivity effects occur at low frequencies[33–37].

In this study, we aimed to define the patterns of functional connectivity that emerge in the human MTL and to specifically characterize how MTL-subregional connectivity differs when memories are being stored versus when they are being subsequently retrieved. We leveraged a large dataset of 108 subjects with depth electrodes placed in the MTL, localized with hippocampal subfield resolution, and focused on three key contrasts: (1) the encoding subsequent memory effect (SME), differentiating remembered from forgotten items, (2) successful retrieval versus unsuccessful memory search, and (3) encoding/retrieval events relative to a non-task baseline. We found that successful encoding was characterized by low-frequency connections which converged on left entorhinal cortex, while retrieval was associated with convergence on left perirhinal cortex. However, these differing connectivity patterns were not correlated with markedly different patterns of local spectral power between encoding and retrieval, suggesting functional connections are a key mechanism by which the MTL may switch between distinct memory operations. Furthermore, during encoding and retrieval, we identified a common network of general task engagement involving left hippocampus and right perirhinal cortex. Taken together, our findings show that low-frequency functional coupling in the MTL supports the formation of new memories, with hippocampus emerging as a hub of general task engagement, but entorhinal and perirhinal cortex acting as the key determinant of successful encoding and retrieval, respectively.

Results

Subsequent memory connectivity

We first set out to determine what patterns of intra-MTL functional connectivity during encoding correlate with successful subsequent memory retrieval. Called the subsequent memory effect (SME), this paradigm has been widely employed to characterize whole-brain modulations of spectral power[29,38] and phase synchrony[3,39] that correlate with successful memory encoding and retrieval. It has also been used to characterize connectivity between specific pairs of MTL subregions[21], but has not been used to create a detailed map of functional connections between all pairs of MTL subregions. In doing so here, our approach allowed us to replicate prior findings of specific intra-MTL synchronization but also broaden the scope to assess the nearly full extent of inter-regional medial temporal connections.

To construct intra-MTL functional connectivity maps, we had 108 subjects perform a verbal free-recall task during which iEEG was collected from depth electrodes placed in the MTL. Subjects were serially presented with 12-item word lists on a screen, and asked to recall as many words as possible after a brief arithmetic distractor task (see Methods for details). For every pair of electrodes in a given subject, we computed inter-electrode coherences at frequencies spanning 4-50 Hz for each of the 1.6-second word encoding intervals (Figure 1A-1C; see Methods for details). Coherence represents the consistency of phase differences between two signals at a given frequency, weighted by the extent to which power in the two signals changes in tandem. As coherence reflects a combined phase-power measure of connectivity during a single time window, it is commonly employed to capture functional connections between iEEG sensors as subjects perform cognitive tasks or during rest[4,6,40,41]. For each electrode pair, the distribution of coherences observed during unsuccessfully recalled items and successful items were compared with a 2-sample T-test, and the resulting t-statistics were then averaged across electrode pairs that spanned a given pair of MTL subregions. Next, t-statistics were averaged

across subjects, yielding a final average t-statistic for a given MTL subregion-pair. To assess for the significance of these average t-statistics, we employed a label-shuffling permutation procedure (Figure 1D; see Methods for details). We first performed this analysis for four broad regions of bilateral MTL: hippocampus, entorhinal cortex (EC), perirhinal cortex (PRC), and parahippocampal cortex (PHC). Region pairs with fewer than 5 subjects contributing electrodes were excluded from analysis (see Supplemental Figure 1 for subject counts per pair).

As several frequency bands have been implicated in intra-MTL synchronization[10,23,34,42,43] – notably theta (4-8 Hz) and low gamma (30-50 Hz) – we first asked how the overall level of SME coherence in the MTL changed as a function of frequency. For each assessed frequency, we computed the z-score that reflects the relative coherence between successfully and unsuccessfully encoded words, averaged across all MTL subregion pairs. Significant coherence was noted in the theta band (permuted $P < 0.05$ at 5 Hz), while significant desynchronization was noted in alpha, beta, and gamma bands (permuted $P < 0.05$ above 9 Hz for several frequencies; see Figure 1E). These findings align with prior observations of enhanced theta synchrony during successful memory encoding – both within the MTL and between cortical regions[3,23] – but refute the notion that gamma underlies inter-regional connectivity within the MTL (for the full adjacency matrix reflecting pairwise gamma SME coherence, see Supplemental Figure 2).

Given our findings of positive theta connectivity, we next set out to determine which specific interactions gave rise to our global measure of enhanced connectivity. As captured by the adjacency matrix representation of intra-MTL connectivity SMEs in the theta band (4-8 Hz), we noted significant coherence between the right hippocampus and PRC ($Z = 5.4$, corrected permuted $P < 0.001$), left EC and left PHC (corrected $P < 0.01$), and marginally significant coherence between the left EC and all other left MTL structures (uncorrected permuted $P < 0.05$

for EC vs. hippocampus, PRC; Figure 2A, 2C). Furthermore, using the node strength statistic – which indicates the overall connectedness of one region to all other regions in the network – the left entorhinal cortex emerged as a significant hub (corrected permuted $P < 0.05$; Figure 2B; for the purposes of node strength computations, we only considered connections to ipsilateral MTL structures due to sparser data for interhemispheric connectivity).

Given our findings of significant hub-like properties in left EC and connectivity to the hippocampus, our precise electrode localizations allowed us to ask which hippocampal subregions contributed to those findings. Using the same coherence SME measure, we computed the z-scored coherence between MTL subregions and each specific subfield of the hippocampus, including CA1, CA3, dentate gyrus (DG) and subiculum (Sub) (see Supplementary Figure 3A for full adjacency matrix). We noted significant SME coupling between the left EC and left Sub (permuted $P = 0.03$; Figure 2C inset), but no other hippocampal structures.

Taken together, our analysis of functional connectivity SMEs in the medial temporal lobe suggest a predominant role for theta interactions (4-8 Hz). Particularly, left EC acts as a hub for intra-MTL connections, while hippocampal-PRC coherence is prominent on the right. These results broadly align with prior findings of hippocampal-rhinal coupling during episodic memory formation in humans[23], and animal models demonstrating hippocampal-entorhinal interaction during memory and navigation[44,45]. Furthermore, we noted significant desynchronization at high frequencies, mirroring similar findings in studies of inter-cortical connectivity during memory[3,39]. To fully characterize the dynamics of the MTL pertaining to episodic memory, two questions remain: (1) What connectivity patterns characterize periods of memory retrieval, in which contextual information is used to cue spontaneous recall, and (2) what do we observe in an SME contrast of spectral power in each MTL region, reflecting local activity?

Connectivity of memory retrieval

Through an analysis of intra-MTL coherences observed during the encoding of word items, we established a predominant pattern of low-frequency connectivity, converging on the entorhinal cortex in the left hemisphere and involving perirhinal cortex on the right. However, memory encoding is only half of the picture – different physiologic processes may underlie memory retrieval, in which context is used to cue reinstatement of information[46]. To examine patterns of theta coherence in the MTL that characterize memory retrieval, we identified all of the 1-second time windows in each subject's recall period that precede onset of a response vocalization, and compared connectivity dynamics against 1-second time windows that are not followed by any vocalization for at least 2 seconds ("unsuccessful memory search"). Procedures are otherwise identical to those described in Figure 1 and Methods section. The result is a connectivity map that reflects how intra-MTL coherence is correlated with successful memory retrieval versus unsuccessful memory search (Figure 3).

In both hemispheres, successful episodic retrieval is associated with strengthened theta connectivity between the hippocampus and PRC (corrected permuted $P < 0.05$, Figure 3A, 3C). Additionally, we further observed interhemispheric connectivity between hippocampus and PRC (corrected permuted $P < 0.05$ for left Hipp. vs. right PRC, left PRC vs. right Hipp.). The left MTL featured significant hippocampal and PRC hubs (corrected permuted $P < 0.05$, Figure 3B), but no significant hubs emerged on the right. These patterns of connectivity during retrieval differ from SME connectivity characterizing encoding; earlier, we noted significant left EC connectivity associated with encoding (Figure 2) but no significant left PRC or hippocampal interconnections. Furthermore, significant interhemispheric coherence was absent in the encoding SME. To tease apart the connectivity between left PRC and hippocampus, we used

detailed electrode localizations to identify significant theta interactions between all hippocampal subfields and left PRC, though the greatest effect size was observed between PRC and DG ($P < 0.001$, $Z = 4.02$; see Supplemental Figure 3B for full adjacency matrix).

Several prior studies of episodic memory have found generally similar spectral power biomarkers between encoding and retrieval contrasts[29,47], but results shown here speak to different underlying patterns of MTL theta connectivity. Since these prior studies did not examine MTL power in detail, it is not known whether we expect to observe similar encoding/retrieval power profiles in our dataset. However, the marked differences in network topology between encoding and retrieval contrasts suggest a reorganization between functional connections underlies switching between memory operations.

Analysis of spectral power

We next asked whether changes in local spectral activity within the MTL correlate with encoding and retrieval states. To do this, we analyzed the relative spectral power between successful and unsuccessful encoding/retrieval trials, in the theta band (4-8 Hz) and frequencies that correspond to high-frequency activity (HFA, 30-90 Hz), established as a general marker of neural activation that likely includes gamma oscillatory components and spectral leakage from aggregate unit spiking activity[48]. For each MTL subregion, we computed the power SME and retrieval contrast for each electrode at each frequency, and averaged these effects across electrodes and subjects (see Methods for details). This procedure results in a t-statistic that reflects the relative power in a given region between successful and unsuccessful encoding/retrieval events.

Though we broadly observed a positive theta connectivity associated with successful memory, spectral power contrasts at the same frequencies went in the opposite direction.

Bilateral CA1 and PRC exhibited significant decreases in theta power associated with successful encoding, as did right DG (corrected $P < 0.05$; Figure 4, upper left). The left MTL exhibited broadly elevated HFA (corrected $P < 0.05$ for all regions except CA3; Figure 4, upper right), while the right MTL saw increases in CA1, Sub and PRC. Example spectrograms for key regions – including left EC and PRC, which exhibited negative theta connectivity SMEs – are depicted in Figure 4 (see Supplemental Figures 4-7 for all spectrograms). The general trend of decreased theta power and increased HFA aligns with a robust literature demonstrating this same effect across a diverse array of cortical regions and the MTL[3,28,29,39].

Notably, while left EC was identified as a hub of theta connectivity during successful encoding, this region did not exhibit a particularly profound theta power SME ($T = -1.66$, $P = 0.13$), though we did observe significantly increased HFA power ($T = 2.73$, $P = 0.013$). Left PRC was a retrieval hub and did exhibit a significant negative theta change associated with retrieval, but no significant increase in HFA (corrected $P > 0.05$). The region with the greatest power SMEs in theta and HFA, left CA1, featured no significant theta connectivity SMEs (corrected permuted $P > 0.05$ for all CA1 connections, see Supplementary Figure 3A).

These results are consistent with a prior investigation of retrieval-related power and synchronization[3], which demonstrated increases in recall-associated theta synchrony associated with decreases in theta power. However, we have shown here that that network hubs in encoding and retrieval periods do not always align with modulations of spectral power; the left EC did not show a significant theta power SME, even as it demonstrated significant increases in theta connectivity. The left PRC exhibited enhanced theta coherence associated with successful recall, but featured no corresponding increase in HFA, which is a marker for local activation (the left PRC did, however show a decrease in theta power).

Encoding vs. non-task condition

Having shown that the most robust positive connectivity effects occur in the theta band, we lastly set out to ask how connectivity dynamics during successful encoding or retrieval differ from periods of no task engagement. This addresses a fundamental gap in much of the literature concerning electrophysiology of human memory: SMEs (or retrieval analogues) only capture the relatively subtle physiologic distinctions between successfully encoded items versus forgotten items. However, in both conditions, memory structures are broadly engaged in a memory task, and even during unsuccessful trials these structures may be contributing to the encoding of previously seen items. Therefore, the SME provides only a sense of fluctuating dynamics on a baseline activation. Here, we set out to characterize that baseline.

To characterize the connectivity dynamics in the MTL relative to a period of no task engagement, we utilized the countdown period prior to the start of a list of words, during which subjects passively watch the screen for 10 seconds. Our statistical procedure is virtually identical to that used to construct the SME contrast, but instead of comparing successful to unsuccessful trials, successful encoding/retrieval events are compared to 1-second surrogate "trials" extracted from the countdown period. Additionally, only the latter 0.5-1.5 second interval of the word encoding period is used, to avoid detecting elevated coherence due to a common event-related potential across electrodes.

As in the SME and retrieval analyses, we first performed this analysis for four broad regions of bilateral MTL: hippocampus, EC, PRC, and PHC. All MTL connections and their associated z-scores are depicted in Figure 5A (significant connections are depicted in Figure 5C). In both encoding and retrieval periods, we found significant connections (corrected permuted $P <$

0.05) between right hippocampus and right PRC. Additionally, we found interhemispheric hippocampus vs. hippocampus, PRC vs. PRC, and left EC vs. right hippocampal coupling.

We used the node strength statistic, computed on ipsilateral MTL connections, to identify left hippocampus and right PRC as hubs of theta connectivity in the encoding versus baseline contrast, and the retrieval vs. baseline contrast (corrected permuted $P < 0.05$; Figure 5B). The presence of identical network hubs in each condition suggests there is similar network structure, relative to baseline, when the MTL is engaged in memory encoding or retrieval. However, SMEs or recall-based contrasts reveal more subtle modulations of connectivity on top of this network that correlate with specific memory operations. These results shed light on the functional low-frequency interactions between different parts of the MTL that generally engage during task performance, but do not necessarily distinguish whether a particular item is successfully encoded or recalled.

Discussion

We set out to understand neural interactions between substructures of the MTL during episodic encoding and retrieval. As 108 subjects performed a verbal free-recall task, we recorded intracranial EEG from the MTL and compared inter-regional coherence between periods of successful and unsuccessful memory operations. Using these methods, we discovered that low-frequency coherence correlates with successful memory encoding and retrieval, with left entorhinal cortex acting as a key hub for theta connectivity during encoding, and left PRC during retrieval. However, during general memory task engagement, we identified theta hubs in the left hippocampus and right PRC, with numerous interhemispheric connections. Concurrent with these dynamics was a general decrease in theta power and increase in high-frequency activity in

both retrieval and encoding, though the degree of power modulation was not predictive of network hubs.

Low-frequency synchronization in the MTL has been conjectured to underlie diverse cognitive operations, including spatial navigation and working memory[10,17]. Under these hypotheses, theta oscillations result in long-term potentiation of synapses in the hippocampus by linking the time of stimulus onset with a cell's state of maximum depolarization. Relatedly, it is well-established that activity in the gamma-band can be modulated by the phase of an ongoing theta oscillation, representing another mechanism that supports inter-regional plasticity[32,49,50]. Our data align with this hypothesis – increases in theta connectivity occurred alongside enhanced HFA in connected areas. We show this theta/gamma dynamic in the context of successful encoding of individual words, suggesting that the cognitive operations which support working memory, navigational memory, and episodic memory are not so different; indeed, episodic encoding of list items is known to involve the contextual binding of one item to another[46], not dissimilar to holding a list in working memory or building a map of a spatial environment[51,20].

Our identification of entorhinal-encoding and perirhinal-retrieval hubs enriches computational models of memory in the MTL. An influential theory of MTL function postulates that theta oscillations within the hippocampal-entorhinal system constitute a common substrate of navigation and episodic memory, by synchronizing EC representations of physical or mental space with hippocampal mechanisms that serve to neurally associate these representations with context (and later serve to retrieve information)[18,19,30]. In support of this theory, we found theta coherence between the left EC and hippocampus in the encoding SME and baseline contrast, concurrent with increased local HFA. Enhanced theta connectivity between EC and PHC, PRC has not been reported before in humans but supports the notion that EC's representations are

built on sensory input from the neocortex, routed through these MTL regions. However, the recall-associated MTL networks organized around PRC are less clearly predicted by this model, which calls for a strong CA1 output to EC[52]. The PRC has long been implicated in retrieval of item-specific information[19,53], and models of free recall predict engagement of mechanisms that support recognition[54], like the PRC. However, the absence of a strong hippocampal-EC connection during recall, in both the retrieval and baseline contrasts, must be reconciled with prevailing theories.

In this study, we failed to find strong evidence for memory-related gamma synchronization within the MTL. This contradicts earlier reports of hippocampal-rhinal gamma connectivity[21,23], some of which may due to methodological differences, such as spectral methods and time windows of interest. However, our finding of significant gamma-band desynchronization – not simply the absence of an effect – raises questions about the extent to which intra-MTL gamma connectivity contributes to successful memory processing. Indeed, we found significant evidence of increased SME power in the gamma band, but this increase was generally associated with decreased coherence. This finding recapitulates an earlier study that utilized a superset of the data here, wherein gamma connectivity was found to decrease during good memory encoding, across a diverse array of cortical regions and hippocampus[3].

Our investigations into the detailed structure of MTL connectivity informs the use of intracranial stimulation to enhance memory. Several recent studies have shown direct entorhinal stimulation in humans either enhances[55–57] or impairs[58] episodic memory encoding. These effects may be mediated through the structural or functional connections of a stimulated region[59], and here we have shown that EC acts a hub of low-frequency connectivity during successful encoding. We note that use of spectral power alone would not have revealed EC as an especially

fruitful target – in fact, a basic ranking of power SMEs would suggest hippocampus as a stimulation target, which has been found to result in memory impairment[60].

In summary, we found that theta band connectivity characterizes intra-MTL interactions that are related to memory encoding and retrieval processes, but distinct networks correlate with successful encoding and retrieval. During encoding, we found EC to be a hub of theta connectivity, with connections to the hippocampus isolated to subiculum. During retrieval, the EC featured weak connectivity, giving way to a hub in PRC. However, both retrieval and encoding were broadly characterized by enhanced HFA and decreased theta power. We introduced the idea of a task vs. baseline contrast, which revealed a network of general task engagement common to retrieval and encoding. These findings point to low-frequency interactions as the key to unlocking the way in which medial temporal structures give rise to episodic memories.

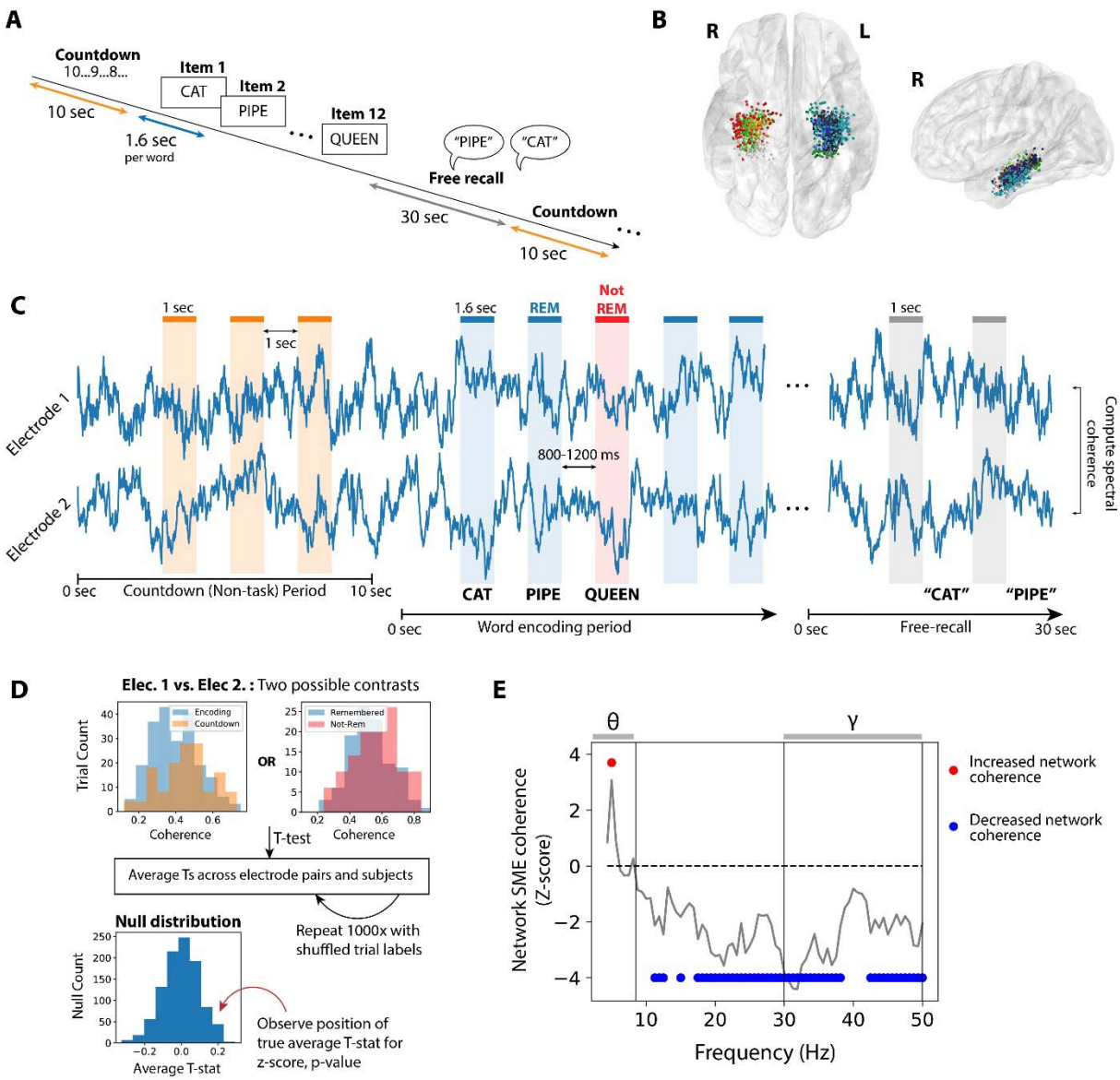

Figure 1. Task structure and analysis methods. A. Subjects performed a verbal free-recall task, consisting of alternating periods of pre-list countdowns (orange), word encoding (blue), and free-recall (gray). See Methods for details. **B.** 108 subjects with indwelling electrodes in the medial temporal lobe (MTL) participated. Electrodes were localized to CA1, CA3, dentate gyrus (DG), subiculum (Sub), perirhinal cortex (PRC), entorhinal cortex (EC), or parahippocampal cortex (PHC). Each dot shows an electrode in this dataset, colored by MTL subregion. **C.** To construct networks of intra-MTL activity, we analyzed spectral coherence between electrode

pairs in frequencies spanning 4-50 Hz. Time windows in three conditions were analyzed: 1-second epochs during the countdown period, to establish baseline connectivity (orange), 1.6-second epochs during word encoding (blue/red), and 1-second periods leading up to recall vocalizations (gray). **D.** To assess the significance of inter-regional coherence, three contrasts were used: a comparison of remembered to not-remembered word events (right panel), a comparison of remembered to baseline events (left panel), or a comparison of recall periods to unsuccessful memory search (not shown; see Methods for details). For each contrast, t-tests were used to measure the relative coherence between conditions for each electrode pair, and t-statistics were then pooled across electrode pairs and subjects. Finally, a label-shuffling permutation procedure was used to generate a null distribution of average t-statistics, from which a p-value or z-score could be derived for each inter-regional pair (see Methods for details). **E.** The average coherence between all possible pairs of MTL regions was compared between successfully encoded and forgotten word items to generate a network-level Z-score, reflecting relative coherence for words that were successfully encoded. This measure was computed for 74 frequencies from 4-50 Hz. Frequencies with significant ($P < 0.05$) overall synchronization are indicated with red markers, while frequencies with significant desynchronization are indicated in blue.

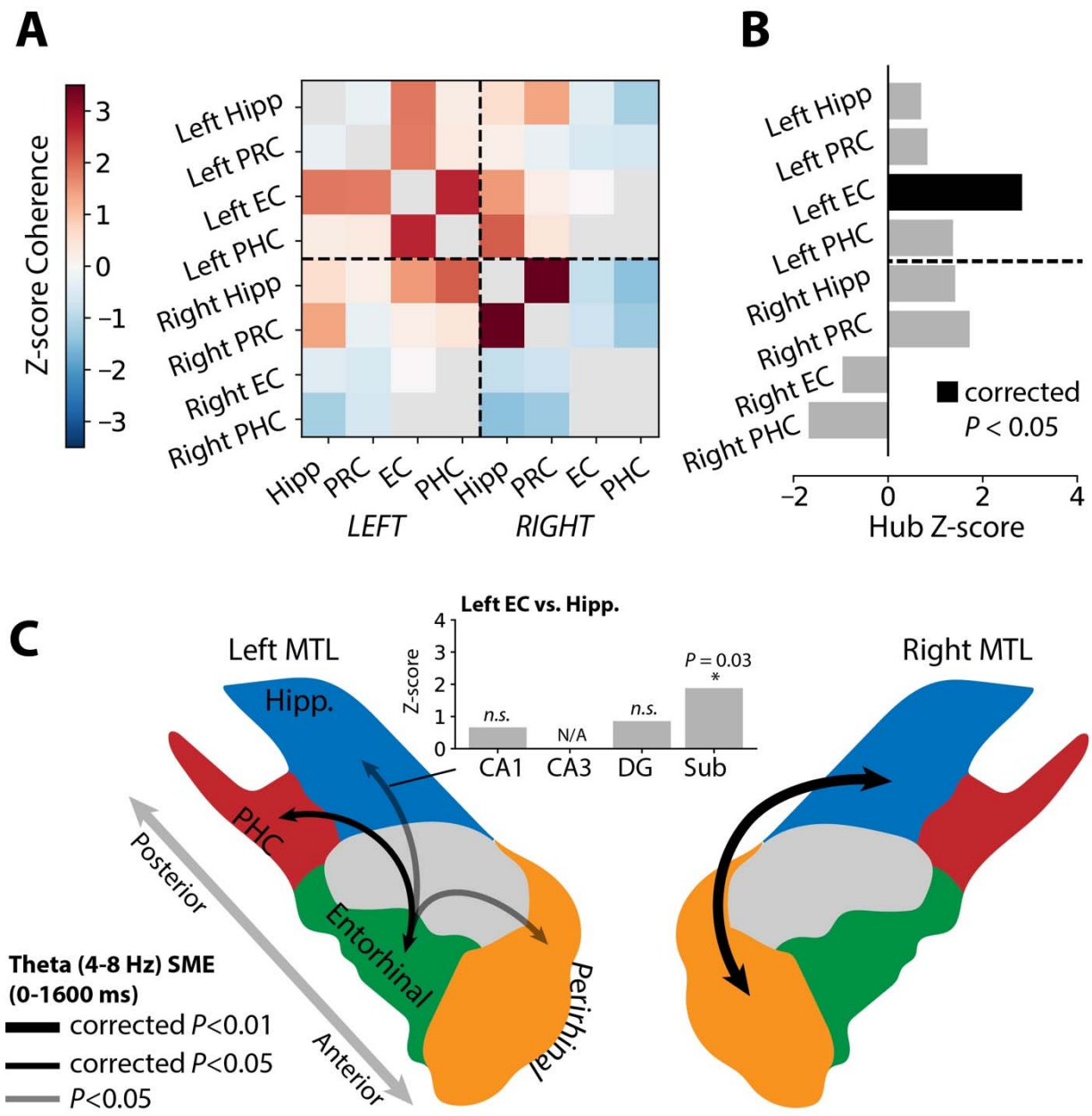

Figure 2. Functional theta (4-8 Hz) connectivity of episodic encoding. A. Adjacency matrix for all assessed intra-MTL connections. Red colors indicate a positive SME connectivity, blue indicated decreased connectivity. Gray shaded cells had fewer than 5 subjects' worth of data, or self-connections that were not assessed (i.e. the diagonal). **B.** Z-scored node strength for each MTL region, computed only for connections to ipsilateral MTL regions (see Methods for details). Node strength indicates the sum of all connections to a given region, with positive Z-

scores indicating enhanced overall connectivity to a given region during successful encoding epochs (a “hub” of connectivity). One region, left entorhinal cortex, exhibited a significant positive node strength (corrected permuted $P < 0.05$). **C.** Schematic of significant theta SME connections, reflecting increased coherence between two MTL regions in successfully encoded versus forgotten word items. Line thickness indicates significance level after FDR correction for multiple comparisons across region pairs (faded lines indicate uncorrected significance if connecting to a hub node, see B). Amygdala, the gray region, was not assessed. Inset bar plot shows breakdown of connections between left EC and hippocampal subfields (see Methods for details on subfield localization). Significant Z-scored theta connectivity SMEs were found between left EC and left subiculum ($P = 0.03$).

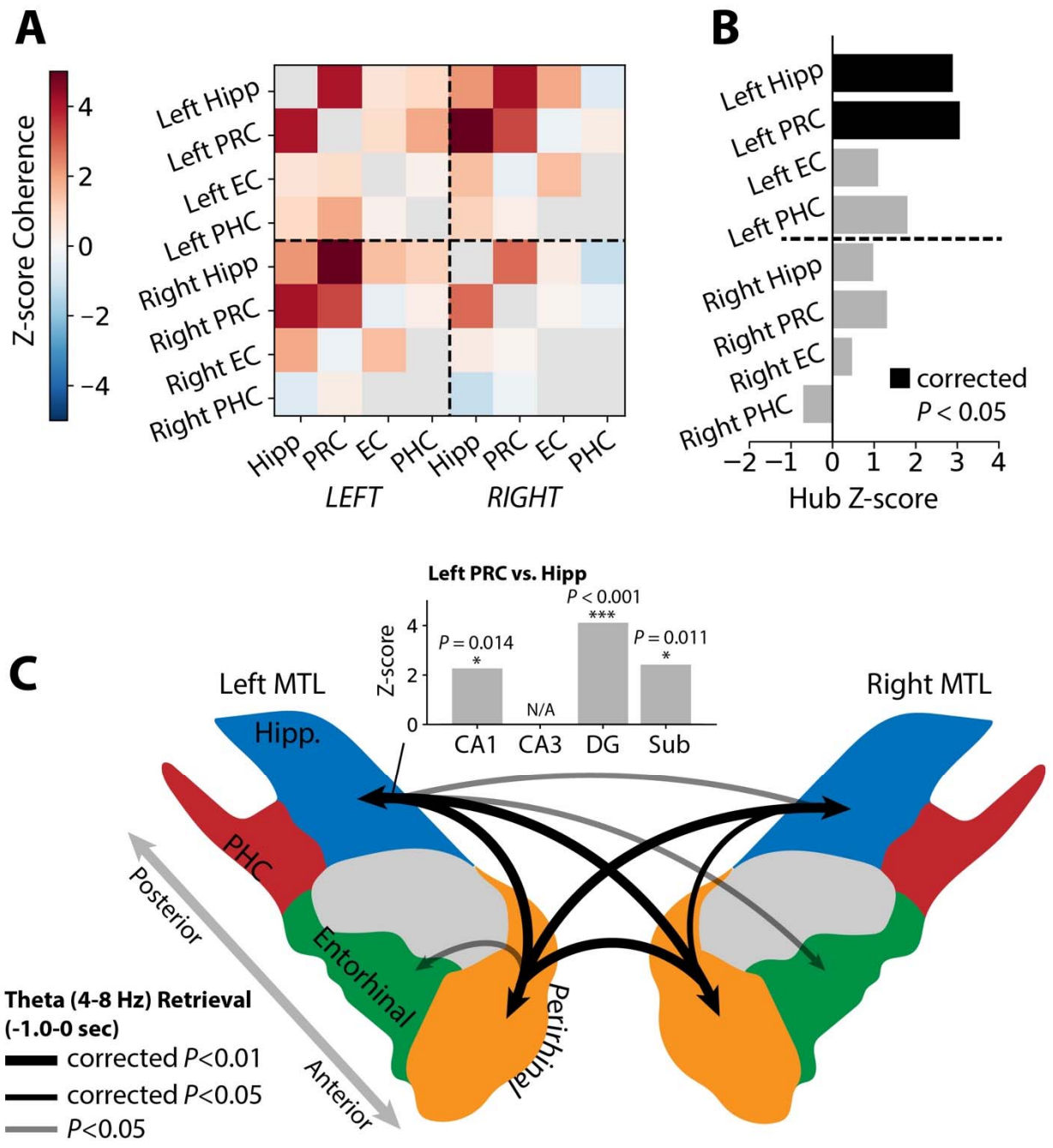

Figure 3. Functional theta (4-8 Hz) connectivity of memory retrieval. A. Adjacency matrix for all assessed intra-MTL connections. Red colors indicate increased connectivity during retrieval periods versus unsuccessful memory search, blue indicated decreased connectivity (see Methods for details). Gray shaded cells had fewer than 5 subjects' worth of data, or self-connections that were not assessed (i.e. the diagonal). **B.** Z-scored node strength for each MTL

region, computed only for connections to ipsilateral MTL regions (see Methods for details). Node strength indicates the sum of all connections to a given region, with positive Z-scores indicating enhanced overall connectivity to a given region during successful encoding epochs (a "hub" of connectivity). Left hippocampus and left PRC exhibited a significant positive node strength (corrected permuted $P < 0.05$) associated with successful retrieval. **C.** Schematic of significant theta retrieval connections, reflecting increased coherence between two MTL regions in the 1 second immediately prior to successful retrieval of a word item. Line thickness indicates significance level after FDR correction for multiple comparisons across region pairs (faded lines indicate uncorrected significance if connecting to a hub node, see B). Inset bar plot shows breakdown of connections between left PRC and hippocampal subfields (see Methods for details on subfield localization). Significant Z-scored theta connectivity was found between left PRC and left CA1, DG, and Sub ($P = 0.014$, <0.001, 0.011, respectively).

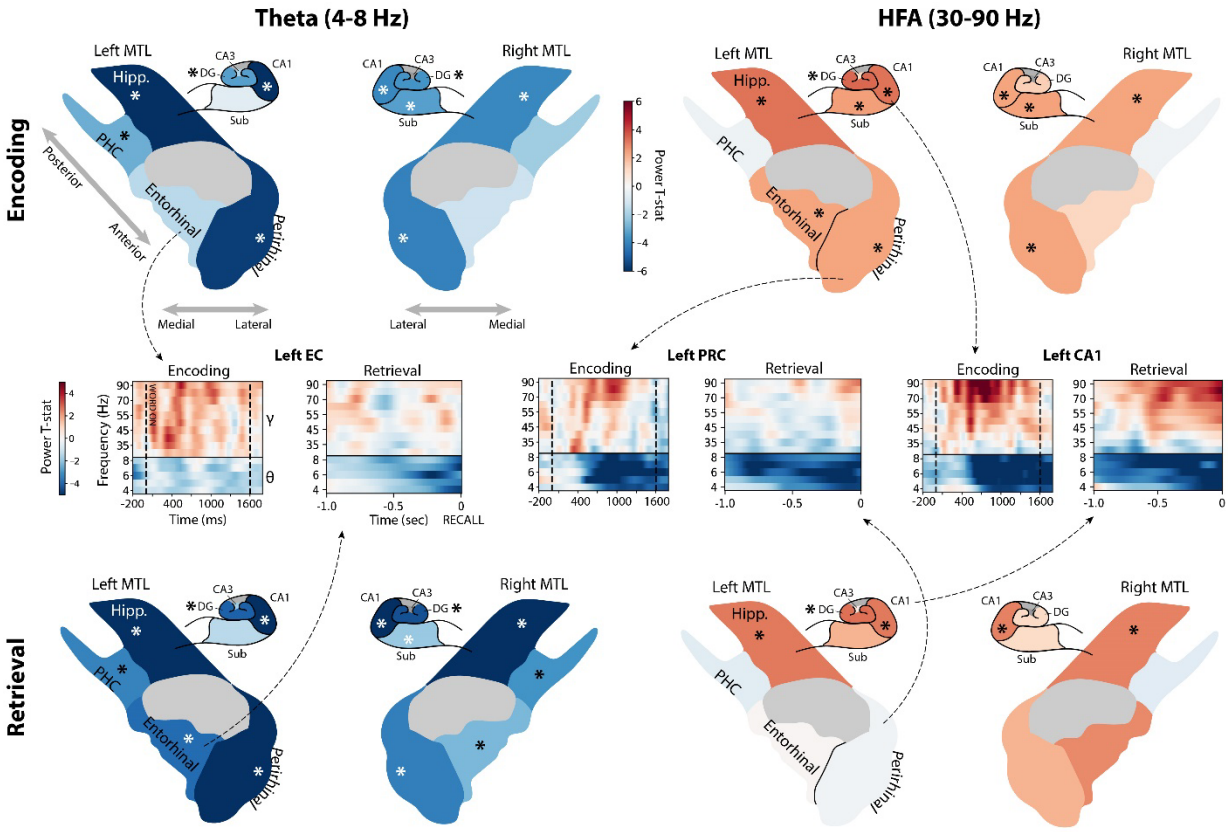

Figure 4. Spectral power dynamics of memory encoding and retrieval. For each MTL subregion and hippocampal subfield, the spectral power during successful vs. unsuccessful encoding or retrieval epochs was computed in the theta (4-8 Hz) and high-frequency activity (30-90 Hz) bands. For encoding periods, powers were averaged in the 400-1100 ms interval, and between -500-0 ms for retrieval periods, which were the periods featuring the most prominent network-wide power change (see Methods for details). The t-statistic indicating the relative power during successful versus unsuccessful encoding or retrieval is mapped to a color, with reds indicating increased power and blues indicating decreased power. These colors are displayed on schematics of MTL and hippocampal anatomy for encoding and retrieval conditions (rows), and theta or HFA bands (columns). Asterisks indicate significant ($P < 0.05$) memory-related power modulation, FDR corrected across tested regions. Centrally, time-frequency

spectrograms are shown for the unaveraged power data in three key regions: left EC, left PRC, and left CA1.

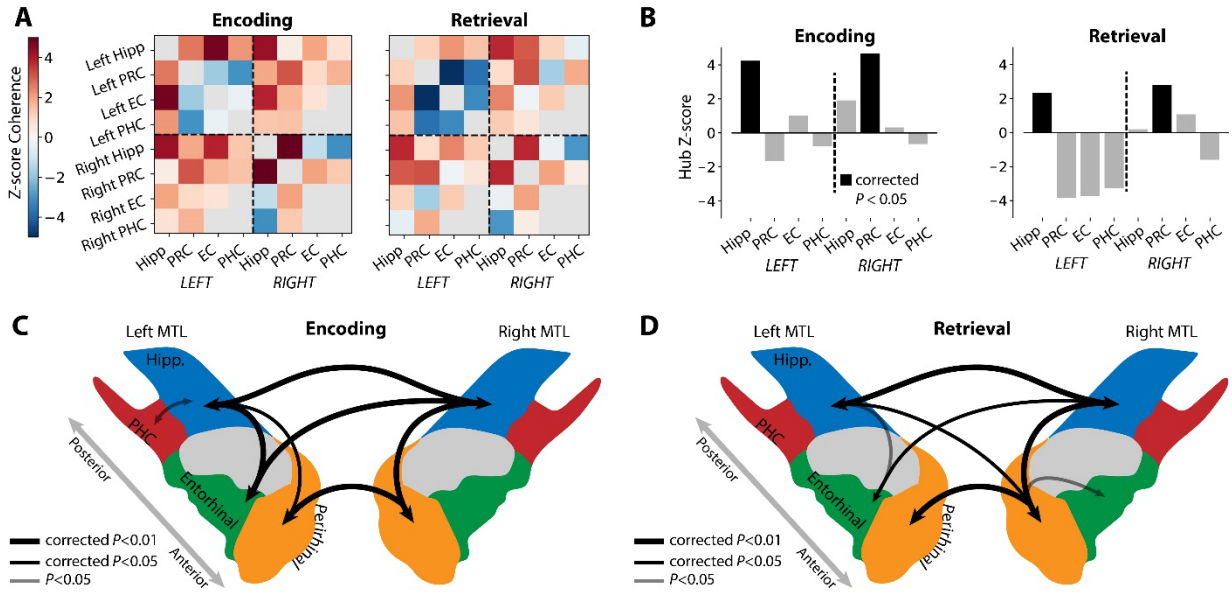

Figure 5. Functional theta (4-8 Hz) connectivity of general task engagement. A. Adjacency matrices for all assessed intra-MTL connections in task versus baseline conditions (left, encoding; right, retrieval). Red colors indicate enhanced coherence during task periods, blue indicates decreased coherence. Gray shaded cells had fewer than 5 subjects' worth of data, or self-connections that were not assessed (i.e. the diagonal). **B.** Z-scored node strength for each MTL subregion, computed only on ipsilateral connections. Node strength reflects the total sum of connections between a given region and all other regions. Left hippocampus and right PRC were FDR-corrected $P < 0.05$ significant hubs in both encoding and retrieval conditions, indicating enhanced connectivity to those regions during general task engagement. **C.** Line thickness indicates significance level after FDR correction for multiple comparisons across region pairs (faded lines indicate uncorrected significance if connecting to a hub node, see B). **D.** Same as C, for the retrieval vs. baseline contrast.

Methods

Participants

For connectivity analyses, 108 patients with medication-resistant epilepsy underwent a surgical procedure to implant subdural platinum recording contacts on the cortical surface and within brain parenchyma. Contacts were placed so as to best localize epileptic regions. Data reported were collected at 8 hospitals over 3 years (2015-2017): Thomas Jefferson University Hospital (Philadelphia, PA), University of Texas Southwestern Medical Center (Dallas, TX), Emory University Hospital (Atlanta, GA), Dartmouth-Hitchcock Medical Center (Lebanon, NH), Hospital of the University of Pennsylvania (Philadelphia, PA), Mayo Clinic (Rochester, MN), National Institutes of Health (Bethesda, MD), and Columbia University Hospital (New York, NY). Prior to data collection, our research protocol was approved by the Institutional Review Board at participating hospitals, and informed consent was obtained from each participant.

Free-recall task

Each subject participated in a delayed free-recall task in which they studied a list of words with the intention to commit the items to memory. The task was performed at bedside on a laptop. Analog pulses were sent to available recording channels to enable alignment of experimental events with the recorded iEEG signal.

The recall task consisted of three distinct phases: encoding, delay, and retrieval. During encoding, lists of 12 words were visually presented. Words were selected at random, without replacement, from a pool of high frequency English nouns (http://memory.psych.upenn.edu/WordPools). Word presentation lasted for a duration of 1600 ms, followed by a blank inter-sitmulus interval of 750 to 1000 ms. Before each list, subjects were given a 10-second countdown period during which they passively watch the screen as centrally-placed numbers count down from 10. Presentation of word lists was followed by a 20 second post-encoding delay, during which time subjects performed an arithmetic task during the delay in order to disrupt memory for end-of-list items. Math problems of the form A+B+C=?? were presented to the participant, with values of A, B, and C set to random single digit integers. After the delay, a row of asterisks, accompanied by a 60 Hz auditory tone, was presented for a duration of 300 ms to signal the start of the recall period. Subjects were instructed to recall as many words as possible from the most recent list, in any order, during the 30 second recall period. Vocal responses were digitally recorded and parsed offline using Penn TotalRecall (http://memory.psych.upenn.edu/TotalRecall). Subjects performed up to 25 recall lists in a single session (300 individual words).

Electrocorticographic recordings

iEEG signal was recorded using depth electrodes (contacts spaced 5-10 mm apart) using recording systems at each clinical site. iEEG systems included DeltaMed XlTek (Natus), Grass Telefactor, and Nihon-Kohden EEG systems. Signals were sampled at 500, 1000, or 1600 Hz, depending on hardware restrictions and considerations of clinical application. Signals recorded at individual electrodes were first referenced to a common contact placed intracranially, on the scalp, or mastoid process. To eliminate potentially confounding large-scale artifacts and noise on the reference channel, we next re-referenced the data using the common average of all depth

electrodes in the MTL that were used for later analysis. Channels exhibiting highly non-physiologic signal due to damage or misplacement were excluded prior to re-referencing.

Anatomical localization

To precisely localize MTL depth electrodes, hippocampal subfields and MTL cortices were automatically labeled in a pre-implant, T2-weighted MRI using the automatic segmentation of hippocampal subfields (ASHS) multi-atlas segmentation method[61]. Post-implant CT images were coregistered with presurgical T1 and T2 weighted structural scans with Advanced Normalization Tools[62]. MTL depth electrodes that were visible on CT scans were then localized within MTL subregions by neuroradiologists with expertise in MTL anatomy. MTL diagrams were adapted with permission from Moore, et al. (2014)[63].

Data analyses and spectral methods

To obtain coherence values between electrode pairs, we used the MNE Python software package[64], a collection of tools and processing pipelines for analyzing EEG data. The coherence (C_{xy}) between two signals is the normalized cross-spectral density (Equation 1); this can be thought of as the consistency of phase differences between signals at two electrodes, weighted by the correlated change in spectral power at both sites.

$$C_{xy} = \left| \frac{S_{xy}}{S_{xx}S_{yy}} \right| \quad (1)$$

Where S_{xy} is the cross-spectral density between signals at electrodes x and y; S_{xx} and S_{yy} are the auto-spectral densities at each electrode. Consistent with other studies of EEG coherence[40,65], we used the multitaper method to estimate spectral density. We used a time-bandwidth product of 4 and a maximum of 8 tapers (tapers with spectral energy less than 0.9 were removed), computing coherence for frequencies between 4-50 Hz, avoiding the 60 Hz frequency range that may be contaminated by line noise. For theta analyses which comprise the majority of this paper, coherence estimates were averaged between 4-8 Hz. For supplemental analyses, gamma was averaged between 30-50 Hz.

To assess the subsequent memory effect (SME) coherence between MTL regions, we computed inter-electrode coherences for each encoding trial during the 1.6-second word presentation window. To assess coherence relative to a pre-task baseline period, we computed inter-electrode coherences for 1.0-second windows during the baseline “countdown” period and compared to 1.0-second windows from 0.5-1.5 seconds during the word presentation interval, to avoid strong effects driven by stimulus onsets. Similarly, 1.0-second memory retrieval intervals were compared to 1.0-second “unsuccessful memory search” windows (see “Retrieval analyses”). Between 4-50 Hz, we extracted 74 frequencies in the 1.6-second windows and 47 frequencies in the 1-second windows.

To ascertain whether there was significant coherence relative to unsuccessful encoding (i.e. the SME) or relative to a non-task baseline, we first computed inter-electrode coherences for all possible pairs of MTL electrodes in each subject, for all trials. For each pair, the distribution of all coherences for all unsuccessful trials was compared to the distribution of successful trials with a 2-sample t-test. T-statistics were then averaged across electrode pairs that spanned a pair

of MTL subregions (either hippocampal subfields or MTL cortices), generating an average t-statistic for each pair of MTL regions in which a given subject had electrodes. Next, t-statistics were averaged across subjects (region pairs with fewer than 5 subjects were not analyzed; see Supplemental Figure 1 for subject counts per pair, which ranged from 5-77).

To assess the significance of these average t-statistics, we used a nonparametric permutation procedure. We shuffled the original grouping of "successful" vs. "unsuccessful" trials and recomputed the grand average SME t-statistics (i.e. across all electrode pairs and subjects) for each of 1000 shuffles. The result is a distribution of null averaged t-statistics, against which the true statistic is compared to generate a z-score or p-value (reported in adjacency matrices in Figures 3, 4, 6-8). Our use of a permutation procedure here obviates the need for variance-stabilizing transformations on coherence values, like a Fisher transformation.

The same statistical procedure was used to compute the difference between encoding and non-task baseline (Figures 6-7) and retrieval vs. unsuccessful memory search, or retrieval vs. non-task baseline (Figure 8).

Network analyses

To visualize networks of intra-MTL connectivity, the z-scored coherence for each MTL pair is depicted as an adjacency matrix, which represents the full set of connections between all nodes (here, MTL regions) in a network. To ascertain which connections are significant among the full set of connections, we Benjamini-Hochberg FDR correct the p-values associated with each connection. To determine which MTL regions act as significant "hubs," or regions that have enhanced connectivity to many other nodes in the network, we use the node strength statistic from graph theory (Equation 2)[66]:

$$k_i^w = \sum_{j \in N} w_{ij} \quad (2)$$

Where k is the node strength of node i, and w_{ij} refers to the edge weight between nodes i and j. N is the set of all nodes in the network. In this paper, we only use ipsilateral MTL regions to compute the node strength of each region, so as to better reflect the engagement of a region with its immediate neighbors. The z-scored connectivity between MTL regions is used as the edge weight. To assess the significance of a hub, we used edge weights derived from each of the 1000 null networks, generated by shuffling the original trial labels (see "Data analyses and spectral methods"). For each region, the true node strength is compared to the distribution of null node strengths to derive a z-score or p-value.

Analysis of spectral power

To determine the change in spectral power associated with successful memory encoding or retrieval, we convolve each electrode's signal with complex-valued Morlet wavelets (5 cycles) to obtain power information. To preprocess the data, we downsampled each signal to 256 Hz and notch filtered at 60 Hz with a fourth-order 2 Hz stop-band Butterworth filter. For theta power, we used 5 wavelets spaced 1 Hz (4-8 Hz), and for high-frequency activity (HFA) we used 13 wavelets spaced 5 Hz (30-90 Hz). For the encoding period analysis, each wavelet was convolved with 4000 ms of data, spanning -1200 ms to 2800 seconds after onset of each word (word

presentation lasts 1600 ms). The leading and trailing 1000 ms are clipped after convolution to remove edge artifacts.

For each electrode in each subject, we log transformed and z-scored power within each session of the free-recall task, which comprises approximately 300 trials. Power values were next averaged into non-overlapping 100 ms time bins spanning the trial. To assess the statistical relationship between power and later recollection of a word (the power SME), power values for each electrode, trial, time, and frequency were separated into two distributions according to whether the word was later or not remembered, a Welch's t-test was performed to compare the means of the two distributions. The resulting t-statistics were averaged across electrodes that fell in a common MTL region (either hippocampal subfields or MTL cortices), generating an average t-statistic per subject. Finally, for all MTL regions with more than 5 subjects' worth of data (all regions except right CA3 met this criteria), we performed a 1-sample t-test on the distribution of t-statistics against zero. The result is a t-statistic that reflects the successful encoding-related change in power across subjects. We report these t-statistics in time-frequency plots in Figure 5B, or, after first averaging power over time and into frequency bands, as barplots in Figure 5A.

Retrieval analysis

To find out whether principles of brain function uncovered in the memory encoding contrast generalize to different cognitive operations, we further analyzed connectivity in a retrieval contrast. This was done in a manner similar to Burke, et al. 2014[29], as follows. For each subject, we identified any 1000 ms interval during the recall period after which no response vocalization occurred for at least 2 seconds, and compared the coherence or power in these "unsuccessful memory search" intervals to the 1000 ms of activity immediately prior to successful item recollection. All other analyses for computing coherence networks or power SMEs were matched exactly with methods described in "Data analyses and spectral methods" or "Analysis of spectral power."

References

1. Eichenbaum, H. A cortical-hippocampal system for declarative memory. *Nat. Rev. Neurosci.* **1,** 41–50 (2000).
2. Paller, K. A. & Wagner, A. D. Observing the transformation of experience into memory. *Trends Cogn. Sci.* **6,** 93–102 (2002).
3. Solomon, E. A. *et al.* Widespread theta synchrony and high-frequency desynchronization underlies enhanced cognition. *Nat. Commun.* **8,** 1704 (2017).
4. Ranganath, C., Heller, A., Cohen, M. X., Brozinsky, C. J. & Rissman, J. Functional connectivity with the hippocampus during successful memory formation. *Hippocampus* **15,** 997–1005 (2005).
5. Vincent, J. L. *et al.* Coherent Spontaneous Activity Identifies a Hippocampal-Parietal Memory Network. *J. Neurophysiol.* **96,** 3517–3531 (2006).
6. Fell, J. & Axmacher, N. The role of phase synchronization in memory processes. *Nat. Rev. Neurosci.* **12,** 105–118 (2011).
7. Eichenbaum, H., Otto, T. & Cohen, N. J. The hippocampus--what does it do? *Behav. Neural Biol.* **57,** 2–36 (1992).
8. Eichenbaum, H., Yonelinas, A. P. & Ranganath, C. The medial temporal lobe and recognition memory. *Annu. Rev. Neurosci.* **30,** 123–52 (2007).
9. Wagner, A. D. *et al.* Building memories: remembering and forgetting of verbal experiences as predicted by brain activity. *Science* **281,** 1188–91 (1998).
10. Buzsáki, G. Theta Oscillations in the Hippocampus. *Neuron* **33,** 325–340 (2002).
11. Moser, E. I., Kropff, E. & Moser, M.-B. Place Cells, Grid Cells, and the Brain's Spatial Representation System. *Annu. Rev. Neurosci.* **31,** 69–89 (2008).
12. MacDonald, C. J., Lepage, K. Q., Eden, U. T. & Eichenbaum, H. Hippocampal 'time cells' bridge the gap in memory for discontiguous events. *Neuron* **71,** 737–749 (2011).
13. Yamamoto, J., Suh, J., Takeuchi, D. & Tonegawa, S. Successful Execution of Working Memory Linked to Synchronized High-Frequency Gamma Oscillations. *Cell* **157,** 845–857 (2014).
14. Montgomery, S. M. & Buzsáki, G. Gamma oscillations dynamically couple hippocampal CA3 and CA1 regions during memory task performance. *Proc. Natl. Acad. Sci. U. S. A.* **104,** 14495–500 (2007).
15. Schomburg, E. W. *et al.* Theta Phase Segregation of Input-Specific Gamma Patterns in Entorhinal-Hippocampal Networks. *Neuron* **84,** 470–485 (2014).
16. Seidenbecher, T., Laxmi, T. R., Stork, O. & Pape, H.-C. Amygdalar and hippocampal theta rhythm synchronization during fear memory retrieval. *Science* **301,** 846–50 (2003).
17. Colgin, L. L. Rhythms of the hippocampal network. *Nature Reviews Neuroscience* **17,** (2016).
18. Hasselmo, M. E. & Eichenbaum, H. Hippocampal mechanisms for the context-dependent retrieval of episodes. *Neural Netw.* **18,** 1172–90 (2005).
19. Diana, R. A., Yonelinas, A. P. & Ranganath, C. Imaging recollection and familiarity in the medial temporal lobe: a three-component model. *Trends Cogn. Sci.* **11,** 379–386 (2007).
20. Burgess, N., Maguire, E. A. & O'Keefe, J. The Human Hippocampus and Spatial and Episodic Memory. *Neuron* **35,** 625–641 (2002).
21. Fell, J. *et al.* Human memory formation is accompanied by rhinal-hippocampal coupling and decoupling. *Nat. Neurosci.* **4,** 1259–64 (2001).

22. Fell, J., Ludowig, E., Rosburg, T., Axmacher, N. & Elger, C. E. Phase-locking within human mediotemporal lobe predicts memory formation. *Neuroimage* **43,** 410–419 (2008).
23. Fell, J. *et al.* Rhinal-hippocampal theta coherence during declarative memory formation: interaction with gamma synchronization? *Eur. J. Neurosci.* **17,** 1082–1088 (2003).
24. Lega, B. C., Jacobs, J. & Kahana, M. Human hippocampal theta oscillations and the formation of episodic memories. *Hippocampus* **22,** 748–761 (2012).
25. Kahana, M. J., Seelig, D. & Madsen, J. R. Theta returns. *Curr. Opin. Neurobiol.* **11,** 739–744 (2001).
26. Hasselmo, M. E. What is the function of hippocampal theta rhythm?--Linking behavioral data to phasic properties of field potential and unit recording data. *Hippocampus* **15,** 936–49 (2005).
27. Lin, J.-J. *et al.* Theta band power increases in the posterior hippocampus predict successful episodic memory encoding in humans. *Hippocampus* **27,** 1040–1053 (2017).
28. Greenberg, J. A., Burke, J. F., Haque, R., Kahana, M. J. & Zaghloul, K. A. Decreases in theta and increases in high frequency activity underlie associative memory encoding. *Neuroimage* **114,** 257–63 (2015).
29. Burke, J. F. *et al.* Theta and high-frequency activity mark spontaneous recall of episodic memories. *J. Neurosci.* **34,** 11355–65 (2014).
30. Buzsáki, G. & Moser, E. I. Memory, navigation and theta rhythm in the hippocampal-entorhinal system. *Nat. Neurosci.* **16,** 130–138 (2013).
31. Buzsáki, G. & Schomburg, E. W. What does gamma coherence tell us about inter-regional neural communication? *Nat. Neurosci.* **18,** 484–489 (2015).
32. Rutishauser, U., Ross, I. B., Mamelak, A. N. & Schuman, E. M. Human memory strength is predicted by theta-frequency phase-locking of single neurons. *Nature* **464,** 903–907 (2010).
33. Watrous, A. J., Tandon, N., Conner, C. R., Pieters, T. & Ekstrom, A. D. Frequency-specific network connectivity increases underlie accurate spatiotemporal memory retrieval. *Nat. Neurosci.* **16,** 349–56 (2013).
34. Colgin, L. L. Mechanisms and Functions of Theta Rhythms. *Annu. Rev. Neurosci.* **36,** 295–312 (2013).
35. Sarnthein, J., Petsche, H., Rappelsberger, P., Shaw, G. L. & von Stein, A. Synchronization between prefrontal and posterior association cortex during human working memory. *Proc. Natl. Acad. Sci. U. S. A.* **95,** 7092–6 (1998).
36. Clouter, A., Shapiro, K. L. & Hanslmayr, S. Theta Phase Synchronization Is the Glue that Binds Human Associative Memory. *Curr. Biol.* **27,** 3143–3148.e6 (2017).
37. Backus, A. R., Schoffelen, J. M., Szebényi, S., Hanslmayr, S. & Doeller, C. F. Hippocampal-prefrontal theta oscillations support memory integration. *Curr. Biol.* **26,** (2016).
38. Burke, J. F. *et al.* Human intracranial high-frequency activity maps episodic memory formation in space and time. *Neuroimage* **85,** 834–843 (2014).
39. Burke, J. F. *et al.* Synchronous and asynchronous theta and gamma activity during episodic memory formation. *J. Neurosci.* **33,** 292–304 (2013).
40. Khambhati, A. N. *et al.* Virtual Cortical Resection Reveals Push-Pull Network Control Preceding Seizure Evolution. *Neuron* **91,** 1170–1182 (2016).
41. Jones, M. W. & Wilson, M. A. Theta Rhythms Coordinate Hippocampal–Prefrontal Interactions in a Spatial Memory Task. *PLoS Biol.* **3,** e402 (2005).

42. Igarashi, K. M., Lu, L., Colgin, L. L., Moser, M.-B. & Moser, E. I. Coordination of entorhinal–hippocampal ensemble activity during associative learning. *Nature* **510,** 143–147 (2014).
43. Fell, J. *et al.* Human memory formation is accompanied by rhinal–hippocampal coupling and decoupling. (2001). doi:10.1038/nn759
44. Yamaguchi, Y. *et al.* A unified view of theta-phase coding in the entorhinal–hippocampal system. *Curr. Opin. Neurobiol.* **17,** 197–204 (2007).
45. Zugaro, M. B., Monconduit, L. & Buzsáki, G. Spike phase precession persists after transient intrahippocampal perturbation. *Nat. Neurosci.* **8,** 67–71 (2005).
46. Howard, M. W. & Kahana, M. J. A Distributed Representation of Temporal Context. *J. Math. Psychol.* **46,** 269–299 (2002).
47. Kragel, J. E. *et al.* Similar patterns of neural activity predict memory function during encoding and retrieval. *Neuroimage* **155,** 60–71 (2017).
48. Burke, J. F. *et al.* Human intracranial high-frequency activity during memory processing: neural oscillations or stochastic volatility? This review comes from a themed issue on Brain rhythms and dynamic coordination. *Curr. Opin. Neurobiol.* **31,** 104–110 (2015).
49. Lisman, J. E. & Jensen, O. The Theta-Gamma Neural Code. *Neuron* **77,** 1002–1016 (2013).
50. Canolty, R. T. *et al.* High Gamma Power Is Phase-Locked to Theta Oscillations in Human Neocortex. *Science (80-.).* **313,** 1626–1628 (2006).
51. Howard, M. W., Fotedar, M. S., Datey, A. V. & Hasselmo, M. E. The Temporal Context Model in Spatial Navigation and Relational Learning: Toward a Common Explanation of Medial Temporal Lobe Function Across Domains. *Psychol. Rev.* **112,** 75–116 (2005).
52. Hasselmo, M. E., Bodelón, C. & Wyble, B. P. A Proposed Function for Hippocampal Theta Rhythm: Separate Phases of Encoding and Retrieval Enhance Reversal of Prior Learning. *Neural Comput.* **14,** 793–817 (2002).
53. Brown, M. W. & Aggleton, J. P. Recognition memory: What are the roles of the perirhinal cortex and hippocampus? *Nat. Rev. Neurosci.* **2,** 51–61 (2001).
54. Lohnas, L. J., Polyn, S. M. & Kahana, M. J. Expanding the scope of memory search: Modeling intralist and interlist effects in free recall. *Psychol. Rev.* **122,** 337–363 (2015).
55. Suthana, N. *et al.* Memory Enhancement and Deep-Brain Stimulation of the Entorhinal Area. *N. Engl. J. Med.* **366,** 502–510 (2012).
56. Titiz, A. S. *et al.* Theta-burst microstimulation in the human entorhinal area improves memory specificity. *Elife* **6,** e29515 (2017).
57. Fell, J. *et al.* Memory Modulation by Weak Synchronous Deep Brain Stimulation: A Pilot Study. *Brain Stimul.* **6,** 270–273 (2013).
58. Jacobs, J. *et al.* Direct Electrical Stimulation of the Human Entorhinal Region and Hippocampus Impairs Memory. *Neuron* **92,** 983–990 (2016).
59. Kim, K., Ekstrom, A. D. & Tandon, N. A network approach for modulating memory processes via direct and indirect brain stimulation: Toward a causal approach for the neural basis of memory. *Neurobiol. Learn. Mem.* **134,** 162–177 (2016).
60. Suthana, N. & Fried, I. Deep brain stimulation for enhancement of learning and memory. *Neuroimage* **85,** 996–1002 (2014).
61. Yushkevich, P. A. *et al.* Automated volumetry and regional thickness analysis of hippocampal subfields and medial temporal cortical structures in mild cognitive impairment. *Hum. Brain Mapp.* **36,** 258–87 (2015).

62. Avants, B. B., Epstein, C. L., Grossman, M. & Gee, J. C. Symmetric diffeomorphic image registration with cross-correlation: Evaluating automated labeling of elderly and neurodegenerative brain. *Med. Image Anal.* **12,** 26–41 (2008).
63. Moore, M. *et al.* A comprehensive protocol for manual segmentation of the medial temporal lobe structures. *J. Vis. Exp.* (2014). doi:10.3791/50991
64. Gramfort, A. *et al.* MNE software for processing MEG and EEG data. *Neuroimage* **86,** 446–460 (2014).
65. Scheeringa, R. *et al.* Neuronal Dynamics Underlying High- and Low-Frequency EEG Oscillations Contribute Independently to the Human BOLD Signal. *Neuron* **69,** 572–583 (2011).
66. Rubinov, M. & Sporns, O. Complex network measures of brain connectivity: Uses and interpretations. *Neuroimage* **52,** 1059–1069 (2010).

Supplementary Information is linked to the online version of the paper at www.biorxiv.org

Acknowledgements We thank Blackrock Microsystems for providing neural recording equipment. This work was supported by the DARPA Restoring Active Memory (RAM) program (Cooperative Agreement N66001-14-2-4032), as well as National Institutes of Health grant MH55687 and T32NS091006. We are indebted to all patients who have selflessly volunteered their time to participate in our study. The views, opinions, and/or findings contained in this material are those of the authors and should not be interpreted as representing the official views or policies of the Department of Defense or the U.S. Government. We also thank Dr. James Kragel for providing valuable feedback on this work.

Author Contributions E.S., M.J.K., and D.S.R. designed the study; E.S. analyzed data, and E.S. wrote the paper. J.S., R. Gorniak, S. Das. performed anatomical localization of depth electrodes. M.S., G.W., B.L., R.G., B.J. recruited subjects, collected data, and performed clinical duties associated with data collection including neurosurgical procedures or patient monitoring.

Data Availability: Raw electrophysiogical data used in this study is freely available at http://memory.psych.upenn.edu/Electrophysiological_Data

Competing Interests
The authors declare no competing financial interests.